J Appl Electrochem (2009) 39:1789–1795
DOI 10.1007/s10800-009-9878-2

ORIGINAL PAPER

Correlation between Cu (I)-complexes and filling of via cross sections by copper electrodeposition

Kazuo Kondo · Taichi Nakamura · Naoki Okamoto

Received: 10 November 2007 / Accepted: 18 March 2009 / Published online: 5 April 2009

Abstract In the manufacture of metal interconnects for semiconductor devices, trenches and vias in dielectric layers on the Si wafer are filled by copper electrodeposition. The acceleration of deposition at the bottom of trenches and vias is a key to the bottom-up filling of these high aspect ratio cavities. We report the detection of this acceleration effect by rotating ring disk electrode experiments. The Cu (I)-complex, which forms on the disk electrode, was captured as a current (I_{ring}) on the ring electrode. I_{ring} increased in periodic reverse pulse current mode, as compared to direct or pulse current. The periodic reverse pulse current produced the most bottom-up filling based on microscopic observations of via cross sections. I_{ring} increased with the additions of Cl^-, which also produced greater bottom-up filling. I_{ring} increased with additions of SPS, which were also found to improve bottom-up filling.

Keywords Copper damascene · Acceleration effect · Rotating ring disk electrode · Cu(I) complex · Via cross section

1 Introduction

The damascene process for the formation of copper on-chip metallization is an important step in the manufacturing of semiconductor devices. In this process, first trench and via cavities are fabricated in a dielectric layer covering the wafer. Then, the trenches and vias are filled by copper electrodeposition over the entire wafer surface. This is followed by a planarization step [1, 2]. The electrodeposition process depends on the additives in the electrolyte. The additives achieve void-free filling of the trenches and vias, by enhancing the deposition rate on the cavity bottom relative to its sidewalls and the outside surfaces. Such bottom-up filling of the electrodeposited copper in the cavities is essential to achieve void-free deposits.

The role of the additive is classified as an inhibition effect outside the vias or trenches and an acceleration effect inside the cavities. The inhibition effect is due to the combination of PEG (polyethylene glycol) and Cl^-. The inhibition effect by PEG and Cl^- has been addressed in a number of studies [3–8]. The acceleration effect is caused by SPS (bis (3-sulfopropyl) disulfide). More recent studies have focused on this acceleration effect, and the influence of SPS has been discussed. Moffat et al. [9–11] attributed the acceleration to the disruption of the inhibition by the sulfonate end group. They proposed the absorption of an accelerator, and a curvature-enhanced mathematical model was proposed which assumes preferential adsorption of the accelerator at the via bottoms due to the concave curvature of this surface. Nekrasov and Berezina [12] used a rotating ring disk electrode and found that the Cu^+ ion is more stable in the presence of Cl^- ion compared to the absence of Cl^- ion. Kondo et al., Vereecken et al. and Okubo et al. studied the acceleration effect using a rotating ring disk electrode, and stated that the acceleration is due to the formation of a stable cuprous (Cu(I)) and SPS complex, such as Cu(I) thiolate and Cu(I)/SPS [13–16]. However, no correlation between the Cu(I)-complex and the electrodeposited via filled cross section was described. Schultz et al. [17] concluded from surface analysis, using in situ surface enhanced Raman scattering (SERS) and infrared-visible sum frequency generation (SFG), that, in the presence of

K. Kondo (✉) · T. Nakamura · N. Okamoto
Department of Chemical Engineering, Osaka Prefecture University, 1-1, Gakuen-chyo, Sakai, Osaka 599-8531, Japan
e-mail: kkondo@chemeng.osakafu-u.ac.jp

Cl^-, a strongly absorbed accelerator (SPS) is not involved in the acceleration reaction. In the present study, the Cu(I)-complex was captured as an oxidation current on the ring electrode. The effects of pulse current waveform, Cl^- additive and SPS additive were investigated, with respect to the formation of the Cu(I)-complex. Also, the correlation of the ring disk electrode results with microscopic observations of Cu(I) filling of via cross sections was examined.

2 Experimental procedure

The basic bath consisted of 0.6 M $CuSO_4 \cdot 5H_2O$ and 1.85 M H_2SO_4. The Cl^- concentrations were 0, 50, 100 and 200 ppm, the PEG (polyethylene glycol, molecular weight 20,000 g/mol) concentration was 400 ppm and the SPS (bis (3-sulfopropyl disulfide)) concentrations were 0, 1, and 10 ppm. With every electrochemical measurement, dissolved oxygen was eliminated by nitrogen sparging for one hour in order to prevent oxidation of the Cu(I)-complexes.

A rotating ring disk electrode (RRDE) was used in the electrochemical measurements. The disk and ring electrodes of the RRDE consisted of glassy carbon, and both electrode areas were 0.2 cm^2. The counter electrode was copper with 0.035 wt% phosphorus and the electrode area was 10 cm^2. The reference electrode was Hg/Hg_2Cl_2 and was connected to the cell by a 0.5 M K_2SO_4 bridge. This reference electrode is referred to as SCE-0.5 M K_2SO_4, as an abbreviation. All experiments were done at room temperature.

Figure 1 is a schematic illustration of the current waveforms applied to the disk electrode. Figure 1a shows the direct current, Fig. 1b the pulse current and Fig. 1c the periodic reverse pulse current. The applied current density was $I_{on} = -20$ mA cm^{-2} for the direct current. For the pulse current, $I_{on} = -20$ mA cm^{-2}, $I_{off} = 0$ mA cm^{-2} and T_{on}:T_{off} = 200:200 ms. For the periodic reverse pulse current, $I_{on} = -20$ mA cm^{-2}, $I_{rev} = 40$ mA cm^{-2}, $I_{off} = 0$ mA cm^{-2} and T_{on}:T_{rev}:T_{off} = 200:10:200 ms. For all waveforms, Cu was initially electrodeposited on the disk electrode until a cathodic charge of 1.2 C cm^{-2} was obtained, and then the I_{ring} measurements were started. The initial electrodeposits were sufficient to cover the glassy carbon disk electrodes with electrodeposited copper. The ring electrodes were kept at the potential of 0.9 V vs. SCE-0.5 M K_2SO_4. The potential of 0.9 V vs. SCE-0.5 M K_2SO_4 is the highest positive potential that did not oxidize the SPS additive [12]. A dual potentiostat (Princeton Applied Research Model 366A) was used, along with a pulse wave generator (Hokuto denko HB-211). The RRDE (Nikko-keisoku SC-5) was rotated at 1,000 rpm. The counter electrode was placed at the cell bottom which was

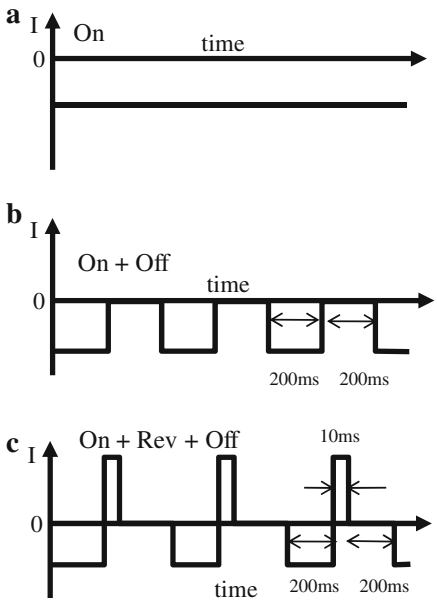

Fig. 1 Schematic illustration of current waveforms. **a** Direct current; **b** Pulse current; **c** Periodic reverse pulse current

4–5 cm from the RRDE electrodes. The reference electrode (Towa denpa HC205C) was located 1 cm from the RRDE electrodes. The ring current (I_{ring}) was recorded using a personal computer.

The via samples consisted of a polyimide film with both sides of the film laminated with copper foil. Vias of 30 μm depth and 50 μm radius were formed on the film. The surface of the film was covered by an electroless copper deposit. This filled via sample was attached to the rotating disk electrode and rotated at 500 rpm. The anode was copper with 0.035 wt% phosphorus, and the electrode area was 15 cm^2. The electrodeposition time was adjusted so that the total deposited charge was 18 C cm^{-2}. The filled via samples were examined by observing their cross sections. The cross sections were formed by initially polishing with emery paper and then 1.0 μm particle diameter Al_2O_3 (Baikowski) as the final polishing step. The filled via cross section was observed by optical microscopy.

3 Results

3.1 Influence of waveforms

Figure 2 shows the relation of I_{ring} (current on the ring of the RRDE) and time for experiments with direct current waveforms. The x-axis is the time measurement in millisecond, and the y-axis is the ring current I_{ring} in μA. Figure 2(a) is I_{ring} from the basic bath, with 100 ppm Cl^-, 400 ppm PEG and 1 ppm SPS as additives. Figure 2(b) is

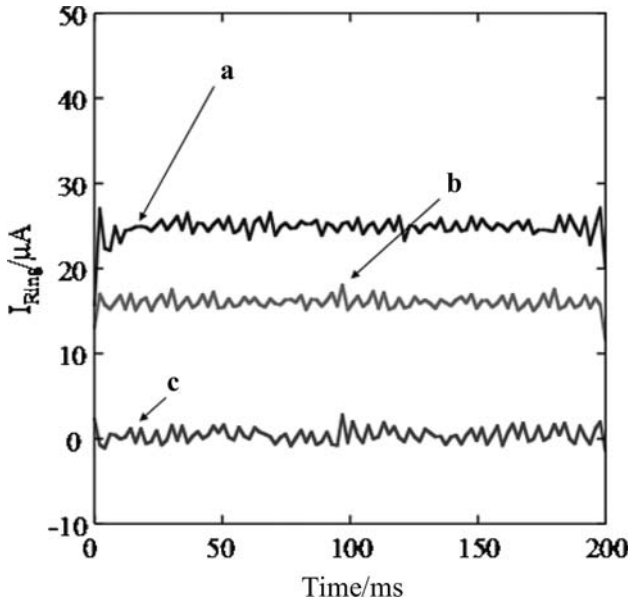

Fig. 2 Ring current vs. time curves for direct current on the disk electrode. (a) Basic bath and Cl^- 100, PEG 400, SPS 1 ppm; (b) Basic bath free of additives; (c) H_2SO_4 bath

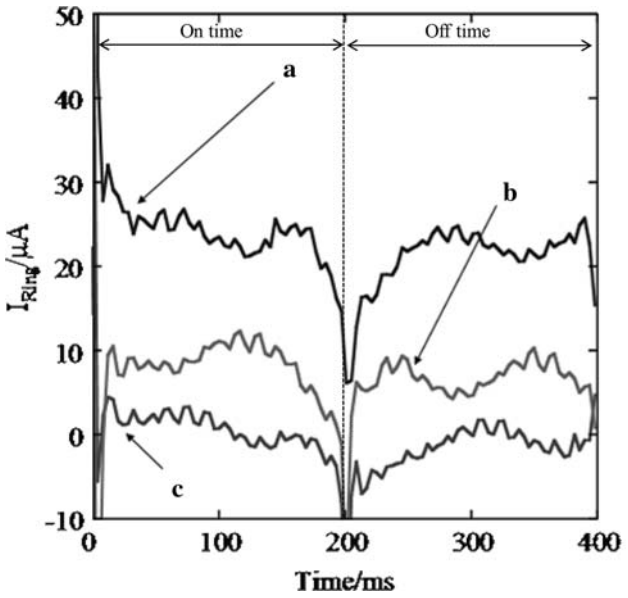

Fig. 3 Ring current vs. time curves for different pulse currents on the disk electrode. (a) Basic bath and Cl^- 100, PEG 400, SPS 1 ppm; (b) Basic bath free of additives; (c) H_2SO_4 bath

I_{ring} for the basic bath without additives, and Fig. 2(c) is that from a bath with only H_2SO_4 and no $CuSO_4$. The difference between the I_{ring} values of (a) and (c) corresponds to the Cu(I)-complexes formed in the basic bath with additives. The difference between the I_{ring} of (b) and (c) corresponds to the Cu(I)-complexes formed in the basic bath with no additives.

Figure 3 shows the relation of I_{ring} and time for experiments with pulse current waveforms. The current on the ring electrode was measured from 0 to 400 ms. The detailed pulse waveform is described in the Experimental procedure section. Figure 3(a) is I_{ring} from the basic bath and 100 ppm Cl^-, 400 ppm PEG and 1 ppm SPS as additives. (b) is that from the basic bath, and (c) is that from only H_2SO_4 not containing $CuSO_4$. The difference between I_{ring} of (a) and (c) corresponds to the Cu(I)-complexes formed in the basic bath with additives. The difference between I_{ring} of (b) and (c) corresponds to the Cu(I)-complexes formed in the basic bath.

Figure 4 shows the relation of I_{ring} and time for the periodic reverse pulse current. The detailed pulse waveform is described in the Experimental procedure section. Figure 4(a) is I_{ring} from the basic bath and 100 ppm Cl^-, 400 ppm PEG and 1 ppm SPS as additives. (b) is that from the basic bath, and (c) is that from only H_2SO_4 without $CuSO_4$. The difference between I_{ring} of (a) and (c) corresponds to the Cu(I)-complexes formed in the basic bath with additives. The difference between I_{ring} of (b) and (c) corresponds to the complexes formed in the basic bath.

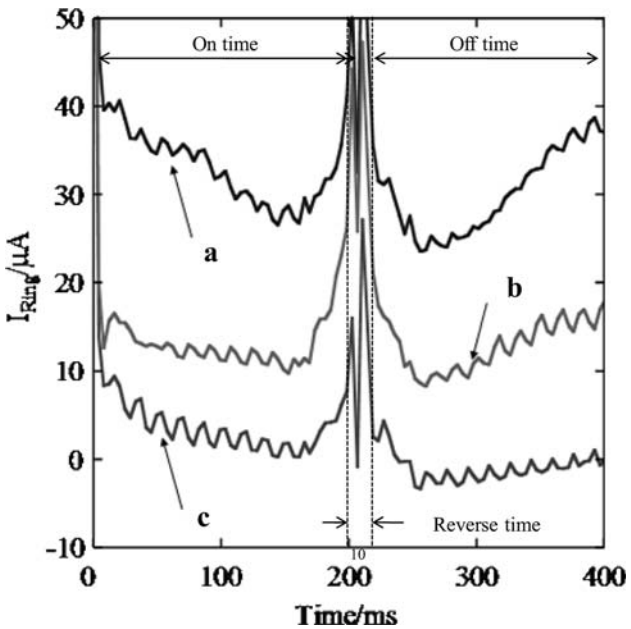

Fig. 4 Ring current vs. time curves for different periodic reverse pulse currents on the disk electrode. (a) Basic bath and Cl^- 100, PEG 400, SPS 1 ppm; (b) Basic bath free of additives; (c) H_2SO_4 bath

Figure 5 shows the relations of I_{ring} and time for the direct current, pulse current and periodic reverse pulse current. Figure 5(a) for the direct current is I_{ring} in Fig. 2(c) subtracted from I_{ring} in Fig. 2(a). Figure 5(b) for the pulse current is of I_{ring} in Fig. 3(c) subtracted from Iring in Fig. 3(a). Figure 5(c) for the periodic reverse pulse current is I_{ring} in Fig. 4(c) subtracted from I_{ring} in Fig. 4(a). The

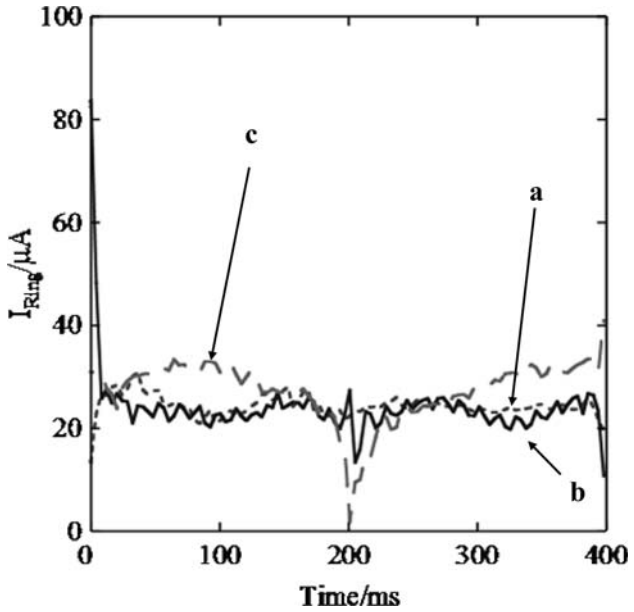

Fig. 5 Ring current and time curves for different current waveforms. (a) Direct current; (b) Pulse current; (c) Periodic reverse pulse current

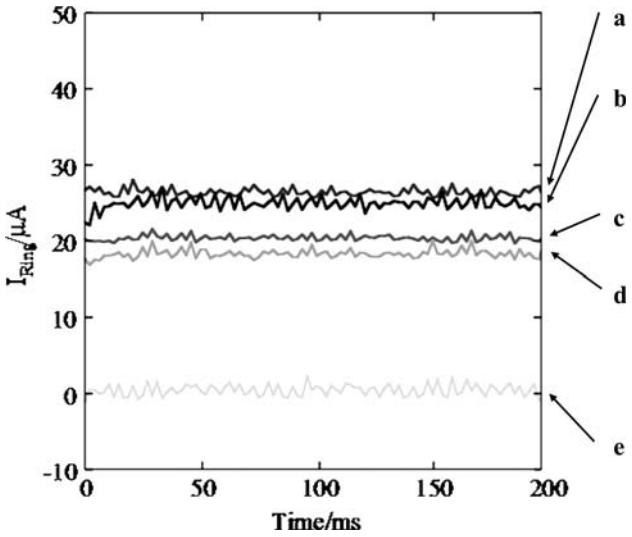

Fig. 6 Ring current vs. time curves for different Cl^- concentrations. (a) Cl^- 200, PEG 400, SPS 1 ppm; (b) Cl^- 100, PEG 400, SPS 1 ppm; (c) Cl^- 50, PEG 400, SPS 1 ppm; (d) Cl^- 0, PEG 400, SPS 1 ppm (e) H_2SO_4 bath

waveform of the periodic reverse pulse current (Fig. 5(c)) has a higher I_{ring}, if compared to the direct current of (a) and the pulse current of (b). This indicates that due to the current reversal, Cu(I)-formation increases in the experiments with the periodic reverse pulse current. During the reverse time (T_{rev}), the copper on the disk partially dissolves and may form the Cu(I)-complexes with Cl^- and SPS.

With the pulse and periodic reverse pulse currents, sudden drops in the current occur at 200 and 210 ms. Since the ring potential (E_{ring}) is kept at 0.9 V vs. SCE-0.5 M K_2SO_4, the ring current (I_{ring}) suffers from an unavoidable sudden change at 200 and 210 ms. I_{ring} should be compared within the stable region and not in the sudden change region of 200 and 210 ms.

3.2 Influence of Cl^- concentration

Figure 6 shows the relation of I_{ring} and time for different Cl^- concentrations. I_{ring} was measured from 0 ms to 200 ms. The applied direct current was $I_{on} = -20$ mA cm^{-2}. The ring voltage was kept constant at 0.9 V vs. SCE-0.5 K_2SO_4. In addition to the basic bath of 0.6 M $CuSO_4 \cdot 5H_2O$ and 1.8 M H_2SO_4, the following additives were added: 200 ppm Cl^-, 400 ppm PEG, and 1 ppm SPS in Fig. 6(a). The additives were 100 ppm Cl^-, 400 ppm PEG, and 1 ppm SPS for Fig. 6(b). The additives were 50 ppm Cl^-, 400 ppm PEG, and 1 ppm SPS in (c) and 0 ppm Cl^-, PEG 400 ppm, and 1 ppm SPS in (d). The bath consisted of only H_2SO_4 in (e). I_{ring} is 0 μA for (e), since no Cu(I)-complex formation occurred without Cu ion in the bath. I_{ring} monotonically increased with increase in the Cl^- concentration from 0 ppm for (d), 50 ppm for (c), 100 ppm for (b) and 200 ppm for (a). This increase in I_{ring} indicates an increase in the Cu(I)-complex concentration, such as $CuCl_2^-$, with the increased Cl^- concentration in the electrolyte. Furthermore, Schulz et al. indicated that the molecular coordination of SPS to a Cu surface in the presence of Cl^- is quite limited, if it occurs at all [16]. This indicates that the existence of Cl^- in the electrolyte prevents adsorption of SPS on Cu and hence promotes the formation of the Cu(I)-complex such as $CuCl_2^-$.

3.3 Influence of SPS concentration

Figure 7 shows the relation of I_{ring} and time for different SPS concentrations. I_{ring} was measured from 0 ms to 200 ms. The direct current was $I_{on} = -20$ mA cm^{-2}. The ring voltage was kept constant at 0.9 V vs. SCE-0.5 M K_2SO_4. In addition to the basic bath of 0.6 M $CuSO_4 \cdot 5H_2O$ and 1.8 M H_2SO_4, the following additives were added: 100 ppm Cl^-, 400 ppm PEG, and 10 ppm SPS in Fig. 7(a); 100 ppm Cl^-, 400 ppm PEG, and 1 ppm SPS in Fig. 7(b); 100 ppm Cl^-, 400 ppm PEG, and 0 ppm SPS in (c). The bath consisted of only H_2SO_4 in (d). I_{ring} is 0 μA for (d), since no Cu(I)-complex formation occurred without Cu ion in the bath. I_{ring} monotonically increased with increase in the SPS concentration from 0 for (c), 1 for (b), and 10 ppm for (a). This increase in I_{ring} indicates an increase in the Cu(I)-complex concentration, such as Cu(I) thiolate, with the increase in the SPS concentration in the electrolyte.

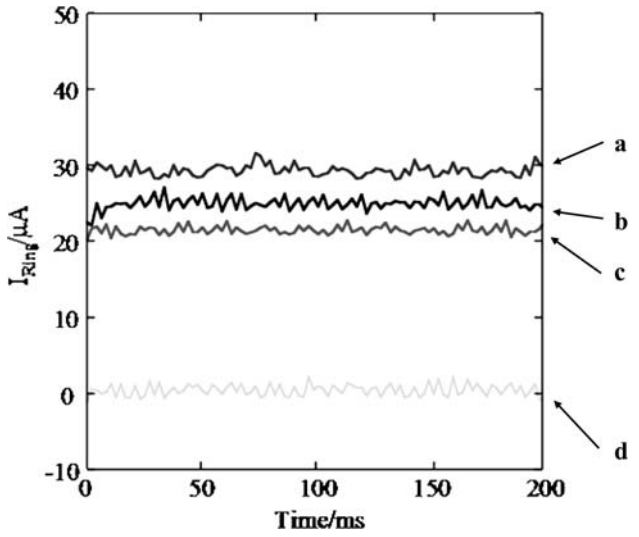

Fig. 7 Ring current vs. time curves for different SPS concentrations. (a) Cl^- 100, PEG 400, SPS 10 ppm; (b) Cl^- 100, PEG 400, SPS 1 ppm; (c) Cl^- 100, PEG 400, SPS 0 ppm; (d) H_2SO_4 bath

3.4 Influence of current waveform on filled cross section

Figure 8 is an optical micrographs of the cross sections of a filled vias with different current waveforms. The black dotted line in Fig. 8a shows the original via geometry. The basic bath consists of 0.6 M $CuSO_4 \cdot 5H_2O$ and 1.85 M H_2SO_4. The additives are 100 ppm Cl^-, 400 ppm PEG, and 1 ppm SPS. The Cu film in Fig. 8a is formed by the direct current of $I_{on} = -20$ mA cm^{-2}. The film in (b) is formed by a pulse current waveform, with $I_{on} = -20$ mA cm^{-2}, $I_{off} = 0$ mA cm^{-2} and T_{on}:T_{off} = 200:200 ms. The Cu deposit in (c) is formed by a periodic reverse pulse current waveform, with $I_{on} = -20$ mA cm^{-2}, $I_{rev} = 40$ mA cm^{-2}, $I_{off} = 0$ mA cm^{-2} and T_{on}:T_{rev}:T_{off} = 200:10:200 ms. The total deposited charge was 18 C cm^{-2} for all current waveforms. As shown in the micrograph, the vias is filled better with the order of direct current (a), pulse current (b) and periodic reverse pulse current (c). Bottom-up filling (shown by the white arrow in Fig. 8a) is observed for the periodic reverse pulse current waveform (c).

3.5 Influence of Cl^- concentration on filled cross section

Figure 9 shows optical micrographs of the cross sections of vias filled using different Cl^- concentrations. A direct current of $I_{on} = -20$ mA cm^{-2} was applied. The basic bath consists of 0.6 M $CuSO_4 \cdot 5H_2O$ and 1.85 M H_2SO_4. The additives are 0 ppm Cl^-, 400 ppm PEG and 1 ppm SPS in Fig. 9a; 50 ppm Cl^-, 400 ppm PEG and 1 ppm SPS in (b); and 100 ppm Cl^-, 400 ppm PEG and 1 ppm SPS in (c). As shown in Fig. 9, bottom-up filling of vias is enhanced by an increasing the Cl^- concentration. The increase in bottom-up filling (shown with black double arrows in Fig. 9c) indicates the increase in the Cu(I)-complex concentration, such as $CuCl_2^-$, due to the increase in the Cl^- concentration in the electrolyte. As indicated by Schultz et al. [16], the existence of Cl^- in the electrolyte prevents adsorption of SPS on the copper and hence promotes the formation of the Cu(I)-complex, such as Cu(I) thiolate.

3.6 Influence of SPS concentration on filled cross section

Figure 10 shows optical micrographs of the cross sections of filled vias, showing the effect of different SPS concentrations. A direct current of $I_{on} = -20$ mA cm^{-2} was

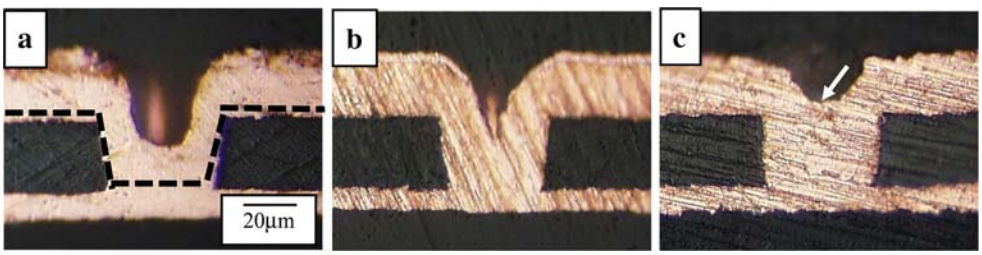

Fig. 8 Cross sectional views of via holes. **a** Direct current; **b** Pulse current; **c** Pulse reverse current

Fig. 9 Cross sectional views of via holes. **a** Cl^- 0, PEG 400, SPS 1 ppm; **b** Cl^- 50, PEG 400, SPS 1 ppm; **c** Cl^- 100, PEG 400, SPS 1 ppm

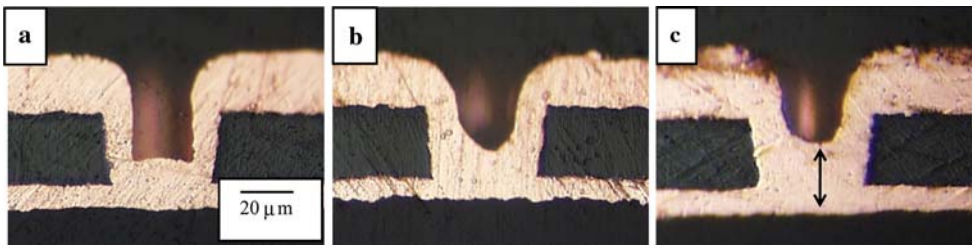

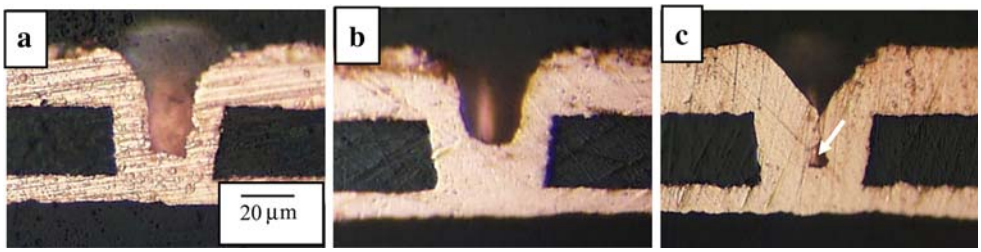

Fig. 10 Cross sectional views of via holes. **a** Cl^- 100, PEG 400, SPS 0 ppm; **b** Cl^- 100, PEG 400, SPS 1 ppm; **c** Cl^- 100, PEG 400, SPS 10 ppm

applied. The basic bath consists of 0.6 M $CuSO_4 \cdot 5H_2O$ and 1.85 M H_2SO_4. The additives were 100 ppm Cl^-, 400 ppm PEG and 0 ppm SPS in Fig. 10a; 100 ppm Cl^-, 400 ppm PEG and 1 ppm SPS in (b); and 100 ppm Cl^-, 400 ppm PEG and 10 ppm SPS in (c). As shown in Fig. 10, bottom-up filled vias is formed with increasing SPS concentration. This increase in the bottom-up filling suggests that the concentration of Cu(I)-complexes, such as Cu(I) thiolate, increase with increase in the SPS concentration in the electrolyte. As indicated by the white arrow in Fig. 10(c), a void exists and bottom-up via filling does not occur. This void may be due to the formation of the Cu(I)-complex, such as Cu(I) thiolate. The Cu(I)-complex formed at both the cathode and anode, other than the via bottom, may form a much thicker copper on the outside of the via compared to the via bottom, and this may form the void seen in Fig. 10(c).

4 Discussion

The formation of the Cu(I)-complex and its reaction will be discussed in this section. Figure 11 shows the formation of the Cu(I)-complexes on the disk electrode and oxidation of the Cu(I)-complexes on the ring electrode. Firstly, Cu(II) ion in the bulk electrolyte reduces to Cu(metal) on the disk electrode.

$$Cu^{2+} + 2e^- \Rightarrow Cu \quad (1)$$

As the side reaction of (1), Cu(II) ion in the bulk electrolyte reduces to Cu(I) on the disk electrode.

$$Cu^{2+} + e^- \Rightarrow Cu^+ \quad (2)$$

$$Cu^{2+} + Cl^- + e^- \Leftrightarrow CuCl_{ad} \quad (3)$$

At the same time, Cu(I) and Cu(II) form complexes with the additives of Cl^-, SPS and the monomer of SPS(MPS). Cu(I) is stabilized by forming Cu(I)-complexes.

$$CuCl_{ad} + Cl^- \Leftrightarrow CuCl_2^- \quad (4)$$

$$4Cu^+ + SPS \Rightarrow 2Cu^{2+} + 2Cu(I)thiolate \quad (5)$$

$$CuCl_{ad} + MPS \Leftrightarrow CuCl\ (thiolate)^- + H^+ \quad (6)$$

$$2Cu + SPS \Rightarrow 2Cu(I)\ thiolate \quad (7)$$

These Cu(I)-complexes formed at the disk reach the ring electrode by convection. The oxidation reactions of the Cu(I)-complexes occur on the ring electrode at 0.9 V vs. SCE-0.5 M K_2SO_4.

$$CuCl_2^- \Rightarrow Cu^{2+} + 2Cl^- + e^- \quad (8)$$

$$Cu(I)thiolate \Rightarrow Cu^{2+} + 1/2SPS + 2e^- \quad (9)$$

$$CuCl(thiolate)^- \Rightarrow Cu^{2+} + 1/2SPS + Cl^- + 2e^- \quad (10)$$

The oxidation reaction of the Cu(I)-complexes on the ring electrode were monitored as I_{ring}.

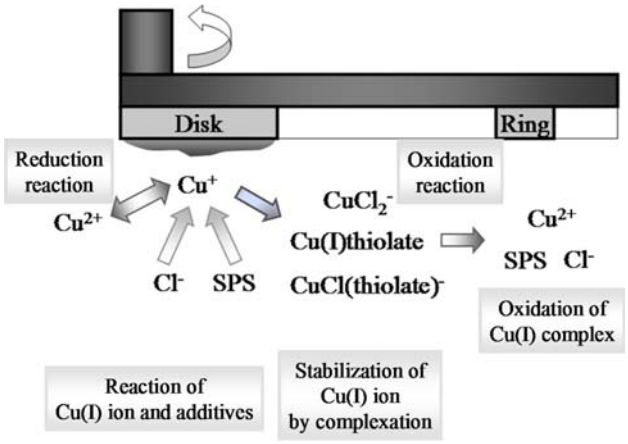

Fig. 11 Schematic illustration of reaction paths at rotating ring disk electrode

5 Conclusions

Cu(I)-complexes formed on the disks of rotating ring disk electrodes during electrodeposition were detected as anodic current on the ring electrode. The effects of the pulse current waveforms of the Cl^- additive and of the SPS additive were investigated with respect to the formation of the Cu(I)-complex. Also, by electrodeposition on samples with via cavities, the effects of the pulse current waveforms, Cl^- additive and SPS additive on filling were examined. It was found that conditions leading to higher ring currents produced improved filling of vias. The results are summarized as follows:

1. A higher amount of Cu(I)-complex formed with periodic reverse pulse current as compared to direct current or pulse current. The ring current increased when periodic reverse pulse current was used. This increase may be due to the formation of the Cu(I)-complex during the pulse reverse T_{rev}. The periodic reverse pulse current results in more bottom-up filling as compared to the direct current and pulse current. This bottom-up filling may be due to the formation of the Cu(I)-complex during the reverse time, T_{rev}.
2. A higher amount of the Cu(I)-complex formed with the addition of Cl^- additive. The ring current increased with the addition of Cl^-. This increase may be due to the formation of a stable Cu(I)-complex such as $CuCl_2^-$. Higher Cl^- concentration resulted in enhanced bottom-up filling of vias, based on the cross section observations. This increase may be due to the formation of a stable Cu(I)-complex, such as $CuCl_2^-$.
3. A higher amount of the Cu(I)-complex formed with the addition of the SPS additive. The ring current increased with the addition of SPS. This increase may be due to the formation of a stable Cu(I)-complex such as Cu(I) thiolate and Cu(I)-SPS. Higher SPS concentrations enhanced bottom up filling, based on the cross section observations. However, a void was present in the cross section of the 10 ppm SPS sample. The Cu(I)-complex formed at both the cathode and anode, rather than the via bottom, and may form a thicker copper layer on the outside of the via compared to the via bottom, and this may be the reason for the void.
4. Corresponding trends of ring current and via filling were obtained with current waveform, Cl^- concentration and SPS concentration. Based on these results, we can reasonably conclude that the acceleration is due to the formation of a stable Cu(I)-complex.

Acknowledgement This study was supported by the Foundation for Technology Promotion of the Electronic Circuit Board.

References

1. Andricacos PC (1999) Electrochem Soc Interface 8:32
2. Andricacos PC, Uzoh C, Dukovic JO, Horkans J, Deligianni H (1998) IBM J Res Dev 42:567
3. Yokoi M, Konishi S, Hayashi T (1983) Denki Kagaku 51:310
4. Reid JD, David AP (1987) Plat Surf Finish 74:66
5. Hebert KR, Adhikari S, Houser JE (2005) J Electrochem Soc 152:C324
6. Stoychev D, Tsvetanov DJ (1996) J Appl Electrochem 26:741
7. Kelly JJ, West AC (1998) J Electrochem Soc 145:3472
8. Jin Y, Kondo K, Suzuki Y, Matsumoto T, Barkey D (2005) Electrochem Solid-State Lett 8:C61
9. Moffat TP, Wheeler D, Josell DJ (2004) J Electrochem Soc 151:C262
10. Moffat TP, Wheeler D, Edelstein M, Josell DJ (2005) IBM J Res Dev 49:19
11. Moffat TP, Wheeler D, Josell DJ (2004) Electrochem Soc Interface 13:46
12. Nekrasov LN, Berezina NP (1962) Dokl Akad Nauk SSSR 142:855
13. Kondo K, Tanaka Z, Yamakawa N (2002) JIEP 5:672
14. Kondo K, Matsumoto T, Watanabe K (2004) J Electrochem Soc 151:C250
15. Vereecken PM, Binstead RA, Deligianni H, Andricacos PC (2005) IBM J Res Dev 49:3
16. Okubo T, Watanabe K, Kondo K (2007) J Electrochem Soc 154:C181
17. Schultz ZD, Feng ZV, Biggin ME, Gewirth AA (2006) J Electrochem Soc 153:C97